An Analytical Behavior On Research For Secure Analysis Of Machine Learning For Multiple Instance Against Standard Supervised Learning

Dr. Amit Kumar Chandanan
Department of Computer Science and Information Technology, Guru Ghasidas Vishwavidyalaya, Bilaspur, India

Abstract:

The drug activity prediction application of the multiple-instance learning model has received a lot of recent attention. The majority of previous research on multiple-instance learning has focused on concept learning; however, the label for drug activity prediction is a real-valued affinity measurement that indicates the binding strength. On Boolean and real-valued data, we investigate the performance of our k-nearest neighbors (k-NN) extensions, Citation-kNN, and diverse density algorithm for the real-valued setting. Additionally, we offer a method for creating artificial data that is chemically accurate.

Keywords:k-NN, Machine Learning,
DOINumber:10.14704/nq.2022.20.8.NQ22985 **NeuroQuantology 2022; 20(8): 9678-9684**

1. INTRODUCTION

Within the field of machine learning, the multiple-instance learning model is gaining in significance. In this model, as opposed to standard supervised learning, in which each instance is labeled in the training data, each example is a set (or bag) of instances with a label indicating whether any one instance in the bag is positive. There is no label given to the individual instances. The learner must come up with a hypothesis that can accurately predict the label of bags that have never been seen before. Take for instance the common problem of learning a Rn-aligned axis-aligned box. Each labeled example in the standard learning model is a point in Rn. drawn using a random distribution called D), and it is marked as positive only if it is in the target box. A collection of points in Rn—commonly referred to as a bag or r-example—is labeled as positive in the multi-instance model if and only if at least one of the points in the bag is in the target box.

The drug activity prediction problem, in which each example is a possible configuration (or shape) for a molecule of interest and each bag contains all low-energy (and thus likely) configurations for the molecule prompted the development of the multiple-instance model. In the application of drug discovery, each bag represents a drug, and the target point represents the ideal shape that will result in the strongest bind with the receptor molecule. Additionally, each point in the bag represents the shapes that the drug is likely to take. One can speed up the process of discovering new

drugs and reduce costs by accurately predicting which molecules will bind to an unknown protein.

The algorithms that we've presented here are very broad. In the training data, B, we assume that each bag has a set of any number of instances, each of which is described by a set of n features. As a result, we can think of this issue as a geometric learning problem in which each bag is a collection of any n-dimensional points. For the drug activity prediction problem, each low-energy conformation typically has one point in the bag. The fact that there is some unknown target point (in the n-dimensional feature space) and the label of a point pi is the inductive bias on which our algorithms are based; The distance between the target point and pi is a function of j that does not increase; j using an unspecified metric. The point in the bag that is closest to the target point serves as the basis for the label on the bag. When using our algorithm, any representation of a molecule as a set of n-dimensional points with this bias would work.

2. PREVIOUS WORK

In the multiple-instance model, three approaches to learning axis-aligned boxes (also known as APR for axis-parallel rectangles) were presented by (1997).In the multi-instance model, they presented three general designs for learning axis-aligned boxes. They began by contemplating the standard algorithm for determining the positive examples' bounds. Additionally, they investigate a noise-tolerant variant of this algorithm. The "outside-in" algorithm was then presented to the audience. In this algorithm, the smallest box that encompasses all positive examples is first constructed, and then this box is reduced to exclude false positives. The "inside-out" algorithm, which starts at a fixed point in the feature space and "grows" a box, was the third one they showed. The idea is to find the smallest box that covers at least one example from each positive bag and none from any negative bag. Then, using statistical methods, they made the box that came out bigger to get better results. On the Musk data set, their algorithm achieves an accuracy of 89 percent when properly tuned.

3. ARTIFICIAL DATA GENERATION

In this section, we explain why we decided to generate artificial data and the method we use to do so. First, we look at how the musk data sets were made. They used uniformly distributed random sampling rays from the origin to create a molecular surface for each conformation by orienting all molecules in relation to a single origin. As a feature value, the length of the molecular surface along each ray was recorded. A 166-dimensional feature vector was created for each conformation by adding additional measurements specific to musk molecules to these 162 features. Dietterich and others obtained Boolean classifications by labeling molecules that a human expert strongly believed to be musk as positive examples and molecules that a human expert strongly believed to be non-musk as negative examples; no "borderline" data was included in this process.

The Lennard-Jones potential, a well-known empirical potential for intermolecular interactions, was used to calculate the artificial molecules' binding energies to the receptor (Berry, 1980).k for a particular feature

$$V_k(r) = 4\varepsilon_k \left(\left(\frac{\sigma}{r}\right)^{12} - \left(\frac{\sigma}{r}\right)^{6} \right) \quad (1)$$

Where ε_k is the depth of the potential well for feature k, $\sigma$is the distance at which $v(r) = 0$. and r_k is the intern clear distance for two monoatomic molecules. One way to think of ek is as a parameter that shows how important a feature is to the binding process, with 1 being the most important and 0 being irrelevant. The Lennard-Jones (LJ) model was chosen for its

ability to qualitatively replicate the actual interaction between molecules and its mathematical simplicity. We assume that s is the same for all features when creating the artificial data. The interaction energy between receptor t and instance B_{ij} on feature $k, E_{Bi,j}$, was calculated using the Lennard-Jones potential (with $r = t_k - B_{i,jk}$) for feature k. The binding energy of $B_{i,j}$ with $t, E_{Bi,j}$was calculated as the sum of $E_{Bi,jk}$ over all features. The binding energy of molecule Bi to t is

$$E_{Bi} = \max_{B_{ij} \epsilon B_i} \left\{ \sum_{k=1}^{n} V(t_k - B_{ijk}) \right\}$$

where n is the number of features.

The label for molecule B_i is the ratio of $E_{Bi}$to the maximum possible binding energy (E_{max}) possible given the artificial receptor and scale factors:

$$LabelB_i = E\,B_i / E_{max}$$

Where $E_{max} = -\sum_{k=1}^{n} \varepsilon_k$. We have obtained one real data set4 that has real-valued affinity values. There are 283 features and 139 bags in this data set, and each bag has an average of 32.5 points. There are only 29 bags with labels that are high enough to be deemed "positive."The labels weren't evenly distributed in the actual data. As a result, the resulting labels also form similar stripes because the feature values of one instance in a molecule were controlled to mimic this behavior during the creation of artificial molecules. To add some diversity, we varied this portion of the generation across the data sets. Our data sets are at www.cs.wustl.edu/sg/multi-inst-data/.

4. DIVERSE DENSITY BASED APPROACH

In this section, we talk about how we improved the real-valued version of Maron and Lozano-Pérez's diverse density algorithm. The diversity density of a point t is, intuitively, nothing more than the likelihood that t is the target in relation to the data. More specifically, the diverse density is a measure of both high positive and low negative instance densities at specific locations.

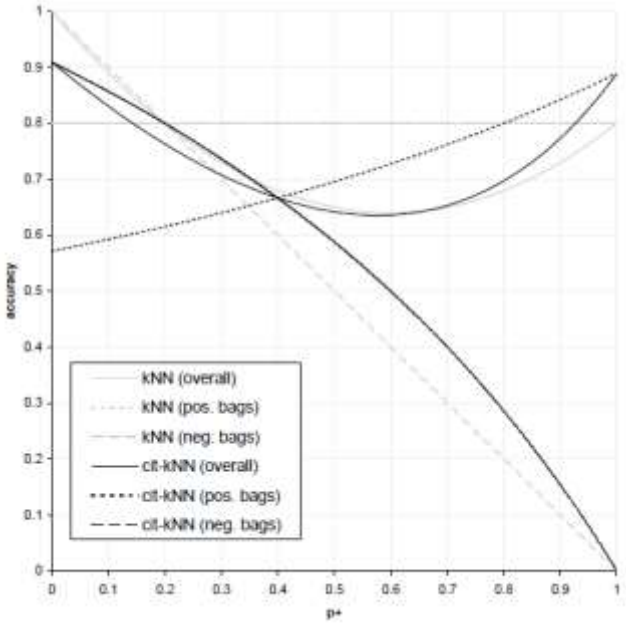

Figure 1 Accuracy of k-NN and citation-kNN for e = 0:2 for the analytical analysis we performed.

in feature space. A high diverse density indicates a good candidate for a "true" concept. Let $B = \{(B_1, l_1), \ldots., (B_i, l_i), \ldots, (B_b, l_b)\}$be the training data. Let B_{ij} denote the j^{th} instance of bag i, and $B_{i,jk}$ denote the feature value of instance $B_{i,j}$ on feature k. The diverse density of possible target point t is defined as

$$DD(t) = \Pr(t/B) = Pr(B/t)\Pr(t)/\Pr(\mathrm{B})\,.$$

We assume uniform priors and so the goal is to search for a t that maximizes $Pr(B/t)$. Assuming the points in B are independent yields

$$PR(B/t) = \prod_{i=1}^{r} Pr\,(B_i/t)$$

By Bayes' rule,

$$\Pr(B_i/t) = Pr(t/B_i)\,\Pr(B_i)/\Pr(\mathrm{t})\,.$$

We assume a uniform prior on the targets and that $Pr(B_i)$ is constant with respect to t. Hence the goal is to maximize $\prod_{i=1}^{b} Pr(t/B_i)$. The key modification required in moving to the real-valued setting is in estimating $Pr(t/B_{ij})$. We let

$$Pr(t/B_i) = (1 - |l_i - Label(B_i/t)|)/Z$$

where $Label(B_{ij}/t)$ is the label $B_i$would receive for target t and Z is a normalization constant.

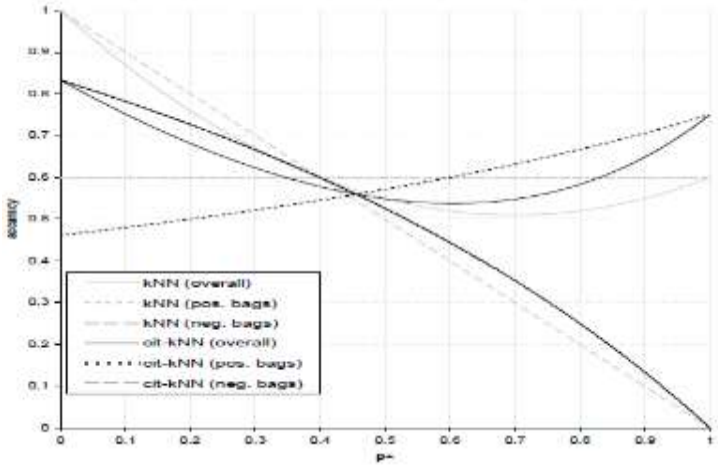

Figure 2 Accuracy of *k*-NN and citation-*k*NN for E= 0:4 for the analytical analysis we performed.

We consider two formulas for $Label\ (B_{ij}/t)$. The first is that of Maron (1999) in which

$$Label\ (B_i/t) = \max_j \left\{ exp\left(-\sum_{d=1}^{n} \left(s_d \left(B_{i,jd} - t_d \right) \right)^2 \right) \right\} \qquad (2)$$

where the target is defined by feature values $t_1 \ldots\ldots\ldots t_n$ and scale factors $s_1 \ldots\ldots\ldots\ s_n$, and the soft max is used to approximate the maximum so that it can be differentiated. If each $l_i \epsilon \{0,1\}$and we use Equation (2), then our algorithm reduces to the standard diverse density algorithm. We also tried used the LJ formula by setting Label $(B_i/t) = E_{B_i}/E_{max}$.

The point t that maximizes $\prod_{i=1}^{b} Pr(t/B_i)$ is found using a gradient ascent search over the 2n dimensional space defined by $t_1 \ldots\ldots\ldots t_n; s_1 \ldots\ldots\ldots\ s_n$ using as multiple starting points the features $t_1 \ldots\ldots\ldots t_n$ from each point in a bag with the maximum label and 0:1 for each s_1.

5 NEAREST NEIGHBOR RESULTS

We begin by providing an overview of the results obtained with the citation k-NN and nearest neighbor algorithms when the number of relevant features and the use of a "strong" data set—one in which there are no examples with labels between 0.36 and 0.77—are varied. The three columns under both citation k-NN and 8-NN display the outcomes of various approaches to selecting the scaling factors that are used to determine the significance of each feature in the distance computation. Both the citation k-NN and nearest neighbor algorithms performed significantly better than the baselines. The NN baseline performed significantly better than the baseline obtained by predicting based on the label of a random bag between the two baselines. We only display the NN baseline for the remaining tables because this relationship is present in all data sets. We tested 2-NN, 8-NN, and citation-kNN (with R=3 and C=5) on these data sets. In terms of prediction error and squared loss, 8-NN outperformed 2-NN by approximately 75%, so we do not report those results. Using the musk data sets, we find that the performance of 8-NN and citation-kNN is very similar, which is very different. For Musk1, citation-kNN has an error of 10.9%, whereas 8-NN has an error of 20.7%.Similarly, citation-kNN has a 14.7% error while 8-NN has a 27.5% error for Musk2.To explain why the musk data sets' results differ from those of our artificial data sets in this regard, additional research is required.

As the number of relevant features grows, the performance dramatically improves, as can be seen in the second half of Table 1.We believe that the fact that most of the features are likely to be relevant and that the musk data set is a "strong" data set contributes in part to the strong performance in terms of the prediction error rate. In the final two rows, we compare the average performance with real values to the average performance with Boolean values (obtained by treating all labels greater than or equal to 0 as negative and the rest as positive).Using real-valued labels significantly reduces the loss, which is not surprising. The fact that using Boolean labels rather than real-valued labels sometimes results in a reduction in prediction error is somewhat surprising. This phenomenon is caused by the fact that when labels of 0 or 1 are used, predictions tend to be off by 1/2, which greatly increases loss but helps keep predictions on the right side of the 0:5 threshold.

The impact of varying the number of degrees of relevance is our next focus. The squared loss for the NN baseline is shown in the leftmost column. The outcomes when the axes are not rescaled (that is, when each feature is considered equally important) are depicted in the subsequent two columns. When our estimation method is utilized to estimate which features are relevant, the performance is shown in the third column. The remaining features are treated equally and the features that are estimated to be irrelevant are left out of the distance calculation. After that, we demonstrate three columns in which the appropriate scale factors for rescaling the axes are calculated by making use of information about the genuine e values. We carry out the procedure that that estimation technique is attempting to accomplish in the column titled "use only relevant."The distance calculation does not take into account any of the irrelevant features, and the remaining ones are treated equally. All features with scale factors of at least 1=2 are used in the column labeled "only use highly relevant."Finally, the axes are rescaled using the true scale factors in the "true scaling" column. As a result, as we move to the right, we use increasingly more in-depth information about the features' true levels of relevance. These last three columns are included to illustrate the potential benefits of accurately estimating scale factors.

*e*ISSN1303-5150

On simpler data sets, 8-NN performs slightly better than 2-NN, but the differences are more pronounced on more complex data sets. The performance of 2-NN and 8-NN are fairly comparable. With three citers and five neighbors, k-NN performs better than 8-NN.The easiest "a" data sets saw improvements when using 5-citers and 3 neighbors, but the other data sets saw a slight decline in performance. The need for citers decreases as the data becomes more clustered and the nearest neighbor provides more information. Lastly, the combination of 10 citers and 8 neighbors performed the best overall.

6. CONCLUDING REMARKS

For the real valued setting, we present extensions of nearest neighbor and various density algorithms in this paper. These algorithms have received some significant insights from our initial research. The number of relevant features has a significant impact on how well the diverse density and nearest neighbor algorithms perform. The performance is quite good when most of the features are relevant, but as a larger portion of the features become irrelevant, it gets worse. The number of relevant features has a greater impact on performance than the number of scale factors, but there is some dependence on this.

REFERENCES

1. Auer, P. (1997), “On learning from mult-instance examples: Empirical evaluation of a theoretical approach”. Proceedings 14th International Conference on Machine Learning, (pp. 21–29), San Francisco: Morgan Kaufmann.
2. Auer, P., Long, P. M. and Srinivasan, A. (1997), “Approximating hyper-rectangles: Learning and pseudo-random sets. Proceedings of the Twenty-Ninth Annual ACM Symposium on Theory of Computing”, (pp. 314–323).
3. Berry, R.S., Rice, S. A. and Ross, J. (1980). “Physical Chemistry”, Chapter 10 (Intermolecular Forces). John Wiley & Sons.
4. Blum, A. and Kalai, A. (1998). “A note on learning from multiple-instance examples. Machine Learning”, 30, 23–29.
5. Dietterich, T. G., Lathrop, R. H. and Lozano-P´erez, T. (1997). “Solving the multiple-instance problem with axis-parallel rectangles. Artificial Intelligence”, 89, 31–71.
6. Fehr, C., Galindo, J., Haubrichs, R. and and Perret, R. (1989). “New aromatic musk odorants: Design and synthesis”. Helvetica Chimica Acta, 72, 1537-1553.
7. Dooly et al, “MultipleInstance Learning of Data”, JMLR Research 2002.
8. Goldman, S.A. and Scott, S.D. (2001). “Multiple-Instance Learning of Real-Valued Geometric Patterns”. To appear in Annals of Mathematics and Artificial Intelligence.
9. Jain, A.N., Dietterich, T.G., Lathrop, R.H., Chapman, D., Critchlow, R.E., Bauer, B.E., Webster, T.A. and Lozano-P`erez, T. (1994). “Compass: A shape-based machine learning tool for drug design”. Computer Aided Molecular Design, 8 635–652.
10. Harikumar Pallathadka, Malik Mustafa, Domenic T. Sanchez, Guna Sekhar Sajja, Sanjeev Gour, Mohd Naved (2021), “Impact of Machine Learning on Management, Healthcare and Agriculture”, Materials Today: Proceedings July 2021.
11. Joseph Futoma, Morgan Simons, Trishan Panch, Finale Doshi-Velez, Leo Anthony Celi (2020), “The Myth of General is Ability in Clinical Research and machine Learning in Health Care”, Lancet Digital Health: 489–92.
12. Karna Vishnu Vardhana Reddy, Irraivan Elamvazuthi, Azrina Abd Aziz, Sivajothi Paramasivam, Hui Na Chua and S. Pranavanand (2021), “Heart Disease Risk Prediction Using Machine Learning Classifiers with Attribute Evaluators”, Appl. Sci. 2021, 11, 8352.

*e*ISSN1303-5150

13. Shahabbodin Shamshirband, Sajjad Hashemi, Hana Salimi, Saeed Samadianfard, Esmaeil Asadi, Sadra Shadkani, Katayoun Kargar, Amir Mosavi, Narjes Nabipour and Kwok-Wing Chau (2020), "Predicting Standardized Stream Flow Index for Hydrological Drought using Machine Learning Models", Engineering Applications of Computational Fluid Mechanics, 2020, VOL. 14, NO. 1, 339–350.